



Ozone deposition to an orange orchard: Partitioning between stomatal and non-stomatal sinks

Silvano Fares^{a,b,*}, Robin Weber^a, Jeong-Hoo Park^a, Drew Gentner^c, John Karlik^d, Allen H. Goldstein^{a,c}

^aUniversity of California, Berkeley, Department of Environmental Science, Policy, and Management, United States

^bAgricultural Research Council (CRA), Research Center for the Soil Plant System, Via della Navicella 2–4, 00184 Rome, Italy

^cUniversity of California, Berkeley, Department of Civil and Environmental Engineering, United States

^dUniversity of California Cooperative Extension, United States

ARTICLE INFO

Article history:

Received 29 November 2011

Received in revised form

18 January 2012

Accepted 21 January 2012

Keywords:

Orange plants

Ozone flux

Stomatal deposition

Non-stomatal deposition

BVOC

ABSTRACT

Orange trees are widely cultivated in regions with high concentrations of tropospheric ozone. Citrus absorb ozone through their stomata and emit volatile organic compounds (VOC), which, together with soil emissions of NO, contribute to non-stomatal ozone removal. In a Valencia orange orchard in Exeter, California, we used fast sensors and eddy covariance to characterize water and ozone fluxes. We also measured meteorological parameters necessary to model other important sinks of ozone deposition. We present changes in magnitude of these ozone deposition sinks over the year in response to environmental parameters. Within the plant canopy, the orchard constitutes a sink for ozone, with non-stomatal ozone deposition larger than stomatal uptake. In particular, soil deposition and reactions between ozone, VOC and NO represented the major sinks of ozone. This research aims to help the development of metrics for ozone-risk assessment and advance our understanding of citrus in biosphere-atmosphere exchange.

© 2012 Elsevier Ltd. All rights reserved.

1. Introduction

Ozone is a principal component of photochemical smog and is also a greenhouse gas. In the polluted lower atmosphere it is formed in the presence of sunlight through photochemical reactions of volatile organic compounds (VOC) with oxides of nitrogen ($\text{NO}_x = \text{NO} + \text{NO}_2$), which have both biogenic (e.g. foliar and soil emissions) and anthropogenic (e.g. evaporative emissions and combustion processes) sources. Due to increasing emissions of anthropogenic air pollutants, background atmospheric ozone concentration in northern mid-latitudes increased substantially in the past few decades (Vingarzan, 2004; Parrish et al., 2009; Cooper et al., 2010). Exposure to elevated ozone concentrations produces biochemical and physiological changes in plants, with inhibition of carbon assimilation by photosynthesis and decreased plant growth being common effects often associated with visible injuries (Wittig et al., 2009; Fares et al., 2006; Vollenweider and Gunthardt-Goerg, 2005; Feng and Kobayashi, 2009). These negative effects result in yield losses that are also transformed into economic losses for crops exposed to high levels of tropospheric ozone. A recent global impact assessment for major agriculture crops estimated annual

production losses of \$US 14–74 billion under present air quality legislation (Van Dingenen et al., 2009).

Plants are natural sinks for ozone (Kurpius and Goldstein, 2003; Fares et al., 2008) and have therefore been argued to phytoremediate the atmosphere (Taha, 1996; Nowak et al., 2006).

The uptake of ozone by ecosystems is attributed to both stomatal and non-stomatal sinks. At the leaf level, stomatal absorption was found to be the major contributor to the total uptake of ozone (Loreto and Fares, 2007; Fares et al., 2010a) and considered to be the main uptake pathway responsible for plant injuries (UNECE, 2004), with stomatal opening mainly influenced by environmental variables such as light, temperature and water availability in the plant-soil system.

Non-stomatal ozone uptake processes include physical deposition to soil, stems, cuticles or any other external surface. Deposition on the cuticles can be limited under dry conditions (Cape et al., 2009), but on wet canopies this process may represent a major sink for ozone (Altimir et al., 2006). Non-stomatal ozone uptake processes also include chemical destruction resulting from gas-phase reactions between ozone and biogenic volatile organic compounds (BVOC) and nitric oxide (NO) emitted from the ecosystem (e.g. plants or soils) (Kurpius and Goldstein, 2003; Fares et al., 2010b). Previous work has reported significant non-stomatal ozone fluxes from forest species owing to reaction with BVOC (Goldstein et al., 2004; Bouvier-Brown et al., 2009; Hogg et al., 2007).

* Corresponding author.

E-mail address: silvano.fares@entecra.it (S. Fares).

Citrus species, in particular orange (*Citrus sinensis*) and mandarin (*Citrus reticulata*), are among the most cultivated tree crops in the Central Valley of California; they accounted for more than 75,000 ha in 2008 (Agriculture Commissioner reports). Citrus is also widely cultivated in other countries with Mediterranean climates, such as Italy, Spain, Morocco, and Israel, and citrus orchards are often close to densely populated areas. The warm climates, along with high insolation required for citrus cultivation, are associated with the formation of high ozone levels when anthropogenic air pollution is also present. In particular, hourly ozone concentrations in the San Joaquin Valley (the southern half of California's Central Valley) often exceed 100 ppb on hot afternoons (California Air Resources Board) which is well above the 40 ppb phytotoxic threshold generally identified for vegetation (UNECE, 2004). Significant emissions of ozone precursors and the topography, heat, and sunshine in the agriculturally rich valleys of California routinely lead to high concentrations of ozone (Howard et al., 2010).

Previously we have reported on experiments using branch enclosures in greenhouses demonstrating the role of *Citrus* leaves in removing ozone via stomatal and non-stomatal processes (Fares et al., 2010a, 2011). For the study reported here, we measured ozone concentration and ecosystem level flux over a complete year for a commercial orange orchard in a region with high concentrations of tropospheric ozone, we partitioned the total ozone flux between stomatal and non-stomatal ozone sinks, and investigated the mechanisms controlling each of these sinks.

2. Material and methods

2.1. Site description

The experimental site was a citrus orchard about three km west of the UC Lindcove Research and Experiment Station (36°21'23.68"N and 119°5'32.14"W), 131 m above sea level. The site is characterized by a Mediterranean climate typical of Central California, with warm dry summers and cool wet winters.

To highlight seasonal differences, we separated the data into three important phenological phases for the orchard: fall-winter, summer, and the flowering period during early spring (DOY 116–145). These periods are well defined by different meteorological conditions and roughly correspond to the low and high ozone periods, with a flowering period which occurs during the transition from low winter to high summer ozone.

Our daily-averaged annual air temperature data (Fig. 1) was similar to the annual air temperature averaged over a period of 12 years as recorded at the CIMIS station

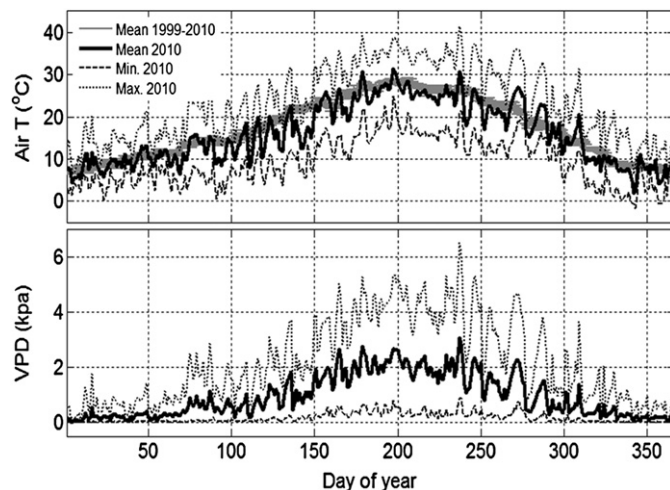


Fig. 1. In black, daily averages of air temperature (upper panel) and vapor pressure deficit (VPD, lower panel) at the citrus research site. The mean 1999–2010 data refer to the average daily temperature (\pm SD) from the CIMIS research station, located at the UC Lindcove citrus research station three km east of our measurement site.

(California Irrigation Management Information System) located at the UC Lindcove research station. Hourly mean values of temperature, vapor pressure deficit, photosynthetically active radiation (PAR) and turbulence (u^*) are shown in Fig. 2, separating between summer, flowering and fall-winter. The typical wind pattern in this area brings daytime air across the valley from the west and then up the mountain slopes of the Sierra Nevada Mountains from the nearby urban area of Visalia, while at night a gentle downslope wind reverses the direction (Fig. 3). The total precipitation over the one-year measurement period was 386 mm, much higher than the annual precipitation averaged for the previous 12 years measured at the CIMIS station (245 ± 132 mm).

The soil texture for the upper horizon (0–33 cm) was loam with a particle size distribution of 42% sand, 38% silt, and 20% clay (Kearney Ag Center). Soil pH was 7.4 (Valley Tech Soil Agricultural Laboratory Services). The orchard was drip-irrigated with water applied twice per week in the warm season to ensure water availability close to field capacity. The site was kept clean from understory vegetation and mechanical pruning operations took place twice a year to limit the size of the orange trees for harvesting and site maintenance.

The block of trees in which the tower and instruments were located was 'Valencia' orange on trifoliate rootstock, with a planting date in the 1960's. The square 4 ha block had dimensions of 200 m N–S and E–W. At the end of the study, we harvested a 'Valencia' citrus tree from within the study block to measure citrus leaf area index (LAI) and biomass density. The tree height was 3.7 m as measured with a telescoping pole. We measured canopy radii in the four cardinal directions to calculate a planar area (as seen from above) of 12.2 m². The mean specific leaf area (SLA) of citrus leaves was 85.4 cm² g⁻¹ obtained by measuring leaf area of five groups of leaf samples with a LiCor Leaf area meter (mod. LI-3100C) followed by drying and weighing. LAI for the orchard was 3.00, derived using the SLA value and the total dry mass of leaves from the harvested tree, multiplied by the plant population of 237 plants per ha as obtained from spacing measurements and Google Maps imagery.

2.2. Experimental set-up

Measurements started in October 2009 and ended in November 2010. For easier comprehension we grouped the data to obtain a continuous time series from day of year (DOY) 1 to DOY 365 by placing 2009 fall observations into the figures after the

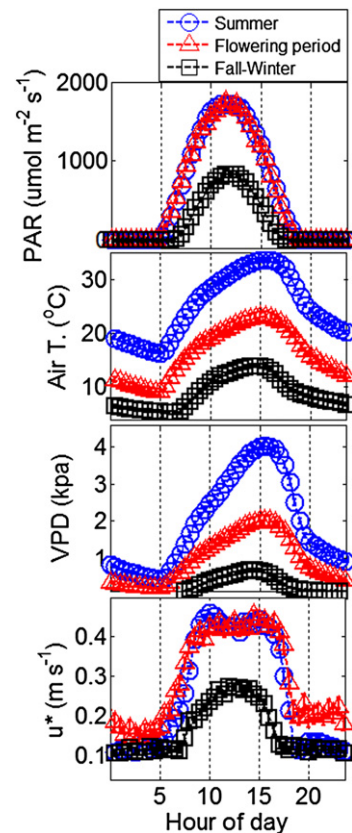


Fig. 2. Hourly mean values (\pm SD) of photosynthetically active radiation (PAR), air temperature, vapor pressure deficit (VPD), and u^* . Data are averaged for the fall-winter, flowering (day of the year 116–145), and summer period.

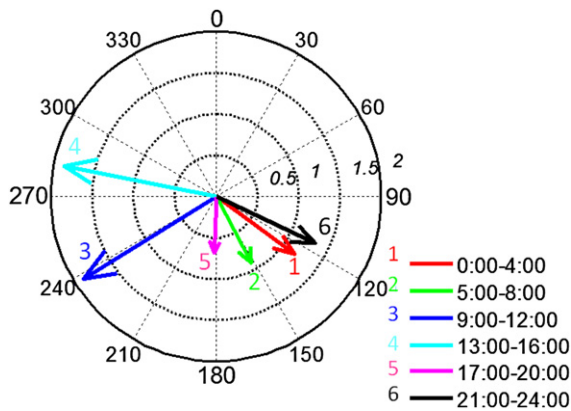


Fig. 3. Wind rose plot with arrows indicating the wind direction (in degrees, 0 = N) for different hours of the day, and x axis showing the wind speed. Data are averaged for the full measurement year.

winter through summer measurements collected in 2010. The experimental facility was composed of an air conditioned shipping container, modified as a field laboratory where analytical equipment was housed, and a measuring tower 9.8 m tall (Floatograph FM50 telescoping mast). The tower was erected on a concrete base between the next two citrus trees west of the field lab. These items were installed in September 2009. The tower was equipped with meteorological sensors, replicated for the top three measuring heights (9.18, 4.85, 3.76 m). A separate tripod was placed between the next pair of trees 7 m west of the tower, and fitted with matching sensors to provide the lowest measuring height of 1.0 m. The measured environmental variables included photosynthetically active radiation (PAR) (Li-Cor Inc., Lincoln, NE), air temperature and relative humidity (Vaisala Inc., Woburn, MA), and soil moisture (Campbell Scientific Inc., Logan, UT). A system of fine wire thermocouples touching the abaxial side of the leaves was used to measure their temperature (Omega Engineering, Precision Fine Wire thermocouples). These data were recorded at 1 min interval using dataloggers (CR10x and CR3000, Campbell Scientific Inc., Logan, UT).

Air was sampled sequentially for 6 min out of every 30 min at four inlet heights through Teflon tubes with 4 mm internal diameter and a Teflon filter (PFA holder, PTFE membrane, pore size 2 μm) located 30 cm from the inlet. Ozone was measured with a UV absorption monitor (1008-PC DASIBI Environmental). The precision of this UV monitor is 1 ppb. In order to avoid different retention times of the air in the inlet lines, tubing was the same length for each inlet line (20 m). The filters were replaced every two weeks to avoid contamination or flow problems. Fast response measurements of ozone were made through a Teflon tube (13 m) and filter inlet located at 7.11 m by chemiluminescence using coumarin dye with an instrument custom developed by the National Oceanic and Atmospheric Administration (NOAA, Silver Spring, MD, Bauer et al., 2000). The chemiluminescence detector was calibrated against 30 min average ozone concentrations from a second UV ozone monitor (1008-PC DASIBI Environmental) which measured air sampled from the same inlet height. Water concentration was measured with a closed path infrared gas analyzer (LI-6262, Lincoln, NE, USA). The raw analog data were recorded at 10 Hz for all gases. Ozone and water concentration were correlated with the vertical wind velocity according to the eddy covariance technique following the methods extensively described in Goldstein et al. (2000), Fares et al. (2010b). Fluxes of gases were calculated according to Eq. (1):

$$F_c = \overline{w' \cdot c'} \quad (1)$$

where w is the vertical wind velocity and c the concentration of the gas. The prime indicates deviations from the 30 min means and the overbar indicates a time average. Wind velocity and sonic virtual temperature fluctuations were measured at 10 Hz with a three-dimensional sonic anemometer (Applied Technologies, Inc., Boulder, CO) mounted on a horizontal beam next to the inlet of the sampling line.

The time lag for sampling and instrument response was determined by maximizing the covariance between vertical wind velocity (w') and scalar (c') fluctuation. Errors due to sensor separation and damping of high frequency eddies were corrected using spectral analysis techniques as outlined by Rissmann and Tetzlaff (1994). The wind data were rotated according to the planar fit method (Wilczak et al., 2001). Data were discarded if: 1. Results from the stationary test for the various were above 60% (Foken and Wichura, 1996); 2. The footprint area was estimated to be outside the boundaries of the orchard (Hsieh et al., 2000); 3. Low turbulence ($u^* < 0.15 \text{ m s}^{-1}$) occurred, which was found during >90% of night hours.

In this work, positive fluxes indicate upward transfer of mass and energy from the ecosystem to the atmosphere, and negative fluxes indicate transfer from the atmosphere into the ecosystem.

2.3. Sap flow systems

Eight sap flow probes using the constant dissipation heat method (mod. TDP 100, Dynamax Inc., Houston, TX) proposed by Granier (1987) were installed in the xylem of 8 tree trunks in the vicinity of the seatainer. For all trees, the radius of the increment core was found to be entirely sapwood (i.e., no heartwood). The average stem radius was 0.1 m, equal to the length of the probes, equipped with 3 thermocouples each (TC) which allowed measurement of sap velocity across three depths of the stem sections. All probes were installed on the northern side of trees to avoid direct solar heating and shielded with aluminum foil to minimize temperature fluctuations in the sapwood. We adopted an empirical relationship proposed by Granier (1985, 1987) to calculate the sap flow velocity (V , cm s^{-1}):

$$V = 0.0119 \cdot \left(\frac{\Delta T_m - \Delta T}{\Delta T} \right)^{1.231} \quad (2)$$

where ΔT ($^{\circ}\text{C}$) is the measured difference in temperature between a heated needle and a reference non-heated needle placed at a fixed distance below the heated one; the parameter ΔT_m ($^{\circ}\text{C}$) is the value of ΔT recorded at night when there is no sap flow (zero set value). A conversion to sap flow rate per unit tree (F ; $\text{g H}_2\text{O s}^{-1}$) was performed by multiplying each V measured at each independent TC level along the probe by the cross-sectional area of sap conducting wood that each TC junction was assumed to measure, similarly to Hatton et al. (1990) and Ford et al. (2004) under the assumption that each TC was measuring a portion of sapwood without overlapping with the adjacent TC.

Leaf transpiration (E_L) was scaled up from mean sap flow rate per tree multiplying by the number of trees per total ground area and dividing by LAI.

Data were logged at 1-min intervals simultaneously with the other meteorological parameters using a datalogger (CR10x, Campbell Scientific Inc., Logan, UT) and successively averaged for 30 min intervals.

2.4. Partitioning of total ozone flux

The total ozone flux (FO_3) measured using the eddy covariance approach was partitioned into a stomatal and several non-stomatal components. Ozone fluxes were related to ozone concentrations through a series of resistances by analogy with an electric circuit obeying Ohm's law (Cieslik, 2004). In this scheme (shown in a diagram by Zhang et al., 2003), stomatal conductance (G_{sto}) from the sap velocity was calculated as the inverse of the stomatal resistance using the Monteith equation (also called Evaporative/Resistance method as reported by previous research (Monteith and Unsworth, 1990; Kurpius et al., 2003; Turnipseed et al., 2009; Gerosa et al., 2007):

$$R_{sto} = \frac{c_p \cdot \rho \cdot \text{VPD}}{\lambda \cdot \gamma \cdot E_L} - (R_a + R_b) \quad (3)$$

where λ is the latent heat of vaporization in air (J kg^{-1}), γ is the psychrometric constant (0.065 kPa K^{-1}), E_L is the transpiration rate ($\text{kg H}_2\text{O m}^{-2} \text{ s}^{-1}$), c_p is the specific heat of air ($\text{J kg}^{-1} \text{ K}^{-1}$), ρ (kg m^{-3}) is density of dry air measured from an RH & T sensor placed at canopy level, VPD is the vapor pressure deficit at leaf level using leaf temperature (kPa), R_a and R_b are aerodynamic and sublayer resistances for water vapor as calculated in Fares et al. (2010b). Stomatal conductance for ozone (G_{O_3}) was calculated correcting G_{sto} for the difference in diffusivity between ozone and water vapor (Massman, 1998). Stomatal ozone (F_{sto}) flux was calculated according to Eq. (4):

$$F_{sto} = G_{O_3} \cdot (O_{3c} - O_{3ci}) \quad (4)$$

We assumed intercellular ozone concentration (O_{3ci}) = 0 (Laisk et al., 1989) so the equation reduces to simply multiplying G_{O_3} by ozone concentration measured at canopy level (O_{3c}). Non-stomatal ozone flux was calculated subtracting F_{sto} to FO_3 . In order to show correlations with temperature and VPD, total, stomatal and non-stomatal ozone fluxes were divided by O_3c to obtain total, stomatal and non-stomatal deposition velocities, respectively O_3Vd , O_3Vd_{sto} and O_3Vd_{nsto} . The canopy conductance to ozone (GcO_3) was calculated from O_3Vd taking into account for R_a and R_b according the following equation:

$$GcO_3 = O_3Vd / (1 - O_3Vd \cdot (R_a + R_b)) \quad (5)$$

Cuticular resistance was calculated according to the deposition model by Zhang et al. (2002) for both wet and dry canopy resistance:

$$R_{cut}(\text{dry}) = \frac{R_{cut}(\text{dry})_0}{e^{0.03 \cdot RH} \cdot LAI^{1/4} \cdot u^*} \quad (6)$$

$$R_{cut}(\text{wet}) = \frac{R_{cut}(\text{wet})_0}{LAI^{1/2} \cdot u^*} \quad (7)$$

Where $R_{cut}(\text{dry})_0$ and $R_{cut}(\text{wet})_0$ are reference values suggested by Zhang et al. (2002) for evergreen deciduous species; RH is the relative humidity measured at canopy level, LAI is leaf area index. We assumed wet conditions when RH was more

than 60% or the leaf wetness sensors placed on the canopy indicated wetness. Fluxes to cuticles were estimated by multiplying the inverse of R_{cut} by O_3c .

Below-canopy resistances were estimated as the sum of in-canopy aerodynamic resistance (R_{ac}) and ground resistance (R_g), calculated according to Erisman et al. (1994), Zhang et al. (2002) and Meszaros et al. (2009):

$$R_{ac} = \frac{14 \cdot LAI \cdot zc}{u^*} \quad (8)$$

$$R_g = 200 + 300 \cdot \frac{SWC}{SWC_{fc}} \quad (9)$$

Where 200 and 300 ($s \text{ m}^{-1}$) are the coefficient and slope of a linear function depending on soil water availability (Meszaros et al., 2009), zc is the canopy height, SWC is the soil water content measured on site and SWC_{fc} is the soil water content at field capacity (0.27) calculated using physical properties of the citrus soil data for the block where orange trees were located, taken from a peer-reviewed website (Kearney Ag Center). Below-canopy ozone fluxes were estimated by multiplying the inverse of ($R_{ac} + R_g$) by ozone concentration measured at the ground level.

Chemical ozone fluxes were calculated after modeling fluxes of BVOC and NO emissions and assuming that 1.0 mol of ozone is removed if it reacts with a BVOC and 0.8 mol of ozone are removed if it reacts with NO (Kurpius and Goldstein, 2003). In particular, BVOC fluxes were calculated using the algorithms proposed by Guenther et al. (1995) with basal emission factor (BEF) related to β -caryophyllene, the main reactive isoprenoid previously reported for Citrus species in Fares et al. (2011):

$$F_{VOC} = BEF \exp[\beta(T - T_s)] \quad (10)$$

Where β ($0.4, \text{K}^{-1}$) is a coefficient that represents the exponential dependence of emissions on leaf temperature (T), and T_s is the leaf temperature at standard conditions (303 K).

For NO fluxes, we used the algorithm proposed by Yienger and Levy (1995) and Steinkamp and Lawrence (2011) using BEF typical of agricultural soils under wet soil conditions of $2.4 \text{ ng(N) m}^{-2} \text{ s}^{-1}$:

$$F_{NO(0^\circ < T \leq 10^\circ C)} = 0.28 \cdot T \cdot BEF \quad (11)$$

$$F_{NO(10^\circ < T \leq 30^\circ C)} = e^{0.103 \cdot T} \cdot BEF \quad (12)$$

$$F_{NO(T > 30^\circ C)} = 21.97 \cdot T \cdot BEF \quad (13)$$

3. Results and discussion

3.1. Meteorology

Meteorological conditions (air temperature, PAR, u^* , VPD) are described in Figs. 1 and 2. These are typical of Mediterranean areas, with daytime summer temperature around 25–30 °C and daytime maxima ranging from 30 °C to 40 °C. Summer daytime VPD was typically 1.5–3 kpa with maxima between 3 and 6 kpa (Fig. 2). Even for this well irrigated orchard, such high VPD caused some stomatal closure on hot days. The site had a regular diurnal pattern of wind flow, with afternoon winds from W–SW and nighttime winds predominately from SE (Fig. 3), thus the footprint of our flux measurements also changed over the course of the day.

3.2. Ozone concentrations

Ozone is a major air pollutant in the Central Valley, where conditions are favorable for its formation due to high sunlight and temperatures, high source strengths of its precursors (NO_x from soil, burning, and mostly from vehicle emissions, VOC from many anthropogenic and biogenic sources), and location in a valley Ozone in this region often exceeds state and federal air quality standards (EPA, 2011; ARB, 2011).

Our data expressed as daily mean, minimum, and maximum (Fig. 4) show ozone concentration in the orchard was high, with daytime peaks typically above 70 ppb in summer, and maximum levels often exceeding 100 ppb. Daytime (10 AM–3 PM) ozone

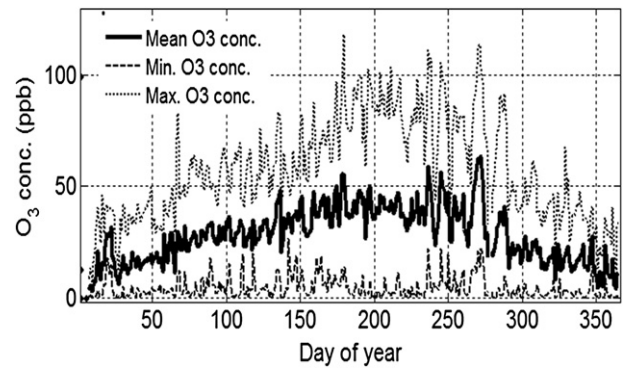


Fig. 4. Daily mean, minimum, and maximum of the ozone concentration measured at the canopy level (O_3c , continuous line). Daily maxima and minima are calculated from 1-min averaged data.

concentration positively correlated with temperature (Fig. 5) as the emissions and chemistry leading to ozone formation in this region are both temperature dependent (e.g. Steiner et al., 2006). We observed regression coefficients (R^2) between ozone and temperature of 0.7 and 0.73 for flowering and summer periods, respectively. Ozone concentrations showed a typical bell-shaped diurnal cycle (Fig. 6), peaking near 3 PM.

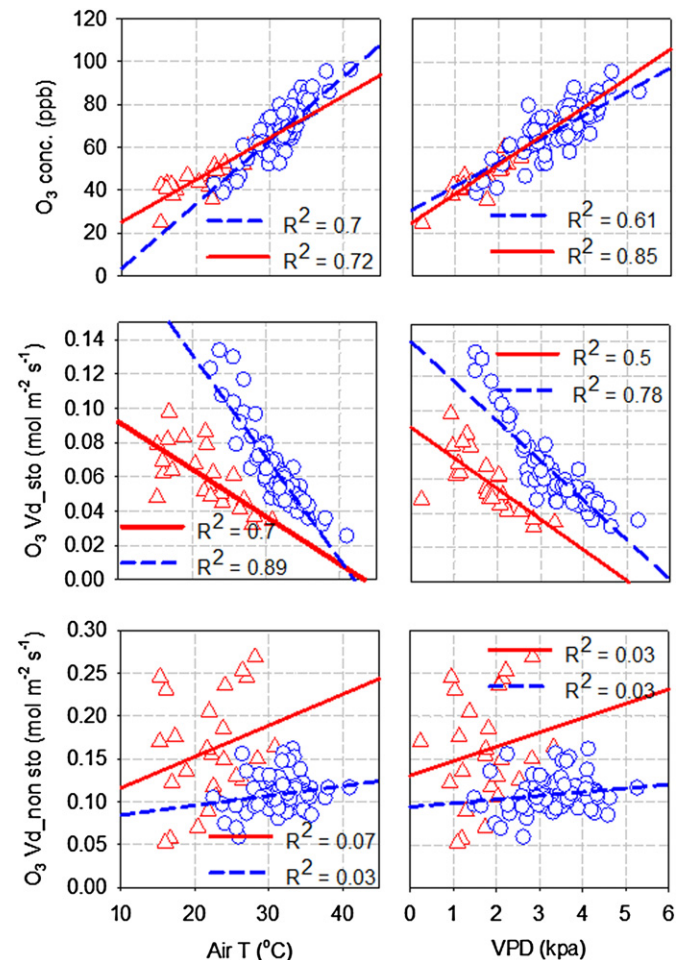


Fig. 5. Correlation of ozone concentration measured at canopy level (O_3c), stomatal ($O_3 Vd_{sto}$) and non-stomatal ($O_3 Vd_{nstn}$) ozone depositions with temperature and vapor pressure deficit. Data are reported for flowering period (triangles) and summer (circles) averaged from 10 AM to 3 PM for each day.

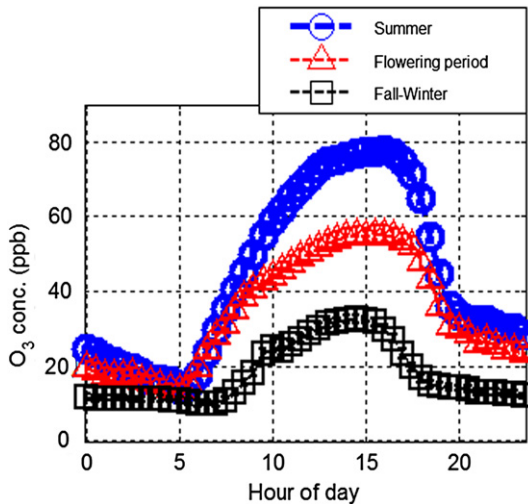


Fig. 6. Hourly average (\pm SD) of ozone concentration measured at canopy level (O_3c) for fall-winter, flowering and summer periods.

The vertical distribution of ozone concentration between the ground and our top measurement height (Fig. 7) was very small during the day and larger at night with lower concentrations near the ground indicating deposition from the atmosphere. Because vertical mixing was much faster during the day, daytime deposition did not result in a strong vertical gradient in concentration, but with slower mixing at night a vertical gradient in concentration was

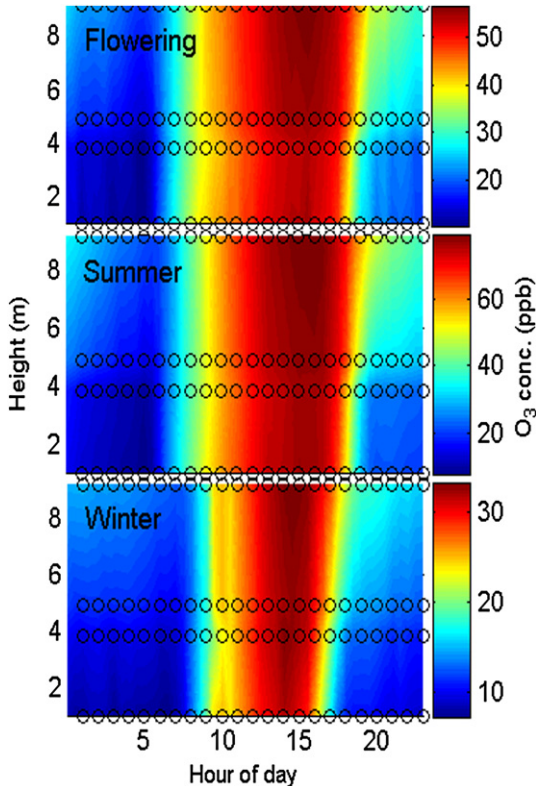


Fig. 7. Hourly average of ozone concentration for fall-winter, flowering and summer periods as a function of height. Measurements were done at 1.0, 3.76, 4.85, and 9.18 m above ground (marked with circles). The canopy height of the orange orchard was 4.0 m. (For interpretation of the references to colour in this figure legend, the reader is referred to the web version of this article.)

routinely observed. This pattern occurred during all seasons demonstrating that ozone deposition takes place at all times during the day and year. Stomatal deposition is typical of daylight hours, due to the well known light-dependence of stomatal aperture, therefore the observed nocturnal vertical gradients provide a clear first indication that non-stomatal deposition phenomena are important ozone sinks in the orange orchard.

3.3. Total ozone fluxes

Total ozone fluxes measured with eddy covariance are reported in Fig. 8 as daily averages, with lowest fluxes in winter and highest fluxes in summer (daily values $\sim 6\text{--}8 \text{ nmol m}^{-2} \text{ s}^{-1}$ in August). A period of high ozone fluxes was also evident during the flowering period (DOY 116–145), with peak values similar to summer conditions even though temperatures were significantly cooler (Fig. 2). This is even more evident from the diurnal average ozone fluxes shown in Fig. 9, where total ozone fluxes during summer and flowering period are shown, with similar values of $\sim 8 \text{ nmol m}^{-2} \text{ s}^{-1}$ during the central hours of the day. Winter fluxes were about half of those measured during summer, as expected considering the temperature dependence of ozone concentration but also the phenology of the plants with lower levels of stomatal conductance during the cold season.

The citrus orchard had a cumulative annual uptake of $7.2 \text{ g m}^{-2} \text{ y}^{-1}$, a value almost identical to that calculated for a forest plantation of *Pinus ponderosa* (Fares et al., 2010a), showing that citrus orchards may be ozone scavengers comparable to forest ecosystems, and demonstrating the ecosystem service orchards can provide through ozone phytoremediation.

3.4. Stomatal ozone fluxes

Stomatal ozone fluxes were calculated by two independent methods that both involved determining ecosystem level transpiration as described in the methods section. First, evapotranspiration measured with eddy covariance was used as an approximation of canopy transpiration and, second, canopy transpiration was measured more directly using sap flow sensors on individual trees. Because this ecosystem had exposed ground and was regularly irrigated, assuming evapotranspiration is approximately equal to canopy transpiration cannot be correct. Indeed, we estimated that soil contributed up to 30% to total evapotranspiration and was therefore not a negligible water source. This estimate was in agreement with results from microlysimeter experiments, in which we installed soil cores in the ground and measured weight loss resulting from evaporated water during successive periods in the five days between two irrigation cycles, as described by Bonachela et al., 1999 (data not shown). Results from these two approaches for estimating stomatal fluxes based on transpiration and VPD are shown in Fig. 8. The estimates based on sap flow measurements performed between DOY 106 and 318 are generally about 30% lower than the estimates based on ecosystem scale evapotranspiration, in agreement with the discussion above showing that $\sim 30\%$ of evapotranspiration was due to evaporation in summer. Therefore, we believe that the second method is more appropriate for this ecosystem, and is hereon used to express stomatal conductance (Fig. 9).

To exclude the effect of ozone concentrations, fluxes were normalized to stomatal and non-stomatal deposition velocities (Fig. 5). Also for our well irrigated ecosystem, the high temperatures, with corresponding high VPD negatively correlated with $O_3 \text{ Vd}_{sto}$ both in flowering and in summer seasons (R^2 between 0.5 and 0.89), a relationship previously observed and tightly connected to the effect of temperature and VPD on stomatal closure

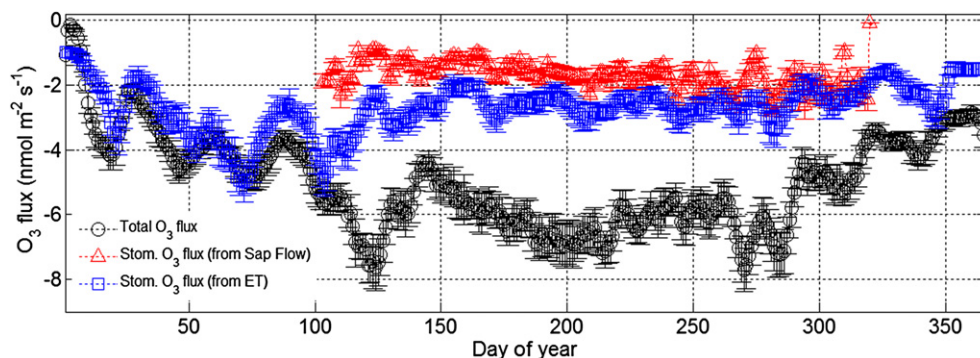


Fig. 8. Daily average (\pm SD) total ozone flux measured with Eddy Covariance (blue line), stomatal ozone flux calculated with the Monteith equation using the water flux measured with Eddy Covariance (green line) and stomatal ozone flux calculated using water flux measured with Sap-Flow sensors. Used from DOY 106 to 318. (For interpretation of the references to colour in this figure legend, the reader is referred to the web version of this article.)

(Fares et al., 2010a). However, light conditions, VPD and air temperature are not independent from each other, as already reported in previous research, since light and VPD affect stomatal aperture and at the same time temperature modulates VPD and drives enzymatic reactions in leaf cells (Turnipseed et al., 2009; Fares et al., 2010a).

In this orange orchard, we studied the relationships between stomatal ($G_{sto} = 1/R_{sto}$) and canopy conductance (G_{cO3}) in order to verify if the latter parameter can be a valid approximation for stomatal conductance during dry and wet conditions. Dry conditions in this study were defined for $RH < 60\%$, a value after which the ratio G_{cO3}/G_{sto} was found to increase with RH, as similarly observed by Lamaud et al. (2009). In these conditions, the low correlation slope of 0.21 ($R^2 = 0.5$, data not shown) from the regression between G_{sto} and G_{cO3} for the entire dataset highlighted divergences between these two parameters, suggesting that G_{cO3} cannot approximate G_{sto} . In conditions of wetness, G_{cO3} was several orders of magnitude greater than G_{sto} . Increase of ozone deposition with wetness has been often observed (Turnipseed et al., 2009; Pleijel et al., 1995; Lamaud et al., 2002) although ozone is known to have low solubility in water. Our data support

the hypothesis raised by Altimir et al. (2006) that water films may modulate chemical reactions with surfaces due to the presence of hydrophobic organic acids. In our site, wet deposition was a recurrent phenomenon due to formation of water puddles after irrigation, dew formation at night on soils and foliage (measured with leaf wetness sensors) due to scarce turbulence that occurred from 11 PM to 6 AM, and precipitation events. However, most nocturnal data ($\sim 90\%$), were removed from calculation since low turbulence ($u^* < 0.15$) did not allow correct calculation of ozone fluxes, while only $\sim 10\%$ of data was excluded during daytime hours.

The long-term measurements of ozone fluxes allowed us to study the seasonality of stomatal ozone fluxes. While total ozone flux was similar during the flowering and summer periods, stomatal fluxes were extremely different, with daytime summer values (above $4 \text{ nmol m}^{-2} \text{ s}^{-1}$, Fig. 9) almost double those of the flowering season. Non-stomatal deposition therefore was much higher during the flowering period than during the summer period.

In a smaller time scale, the diurnal cycles of ozone concentration and ozone flux were slightly different, with maximum ozone concentration occurring after 3 PM during summer, and maximum ozone fluxes occurring before 3 PM. This phenomenon has been previously described for a ponderosa pine forest (Kurpius and Goldstein, 2003; Fares et al., 2010c) and was confirmed in our study to also occur in the orange orchard. This is the result of stomatal closure in the late afternoon (data not shown), reducing stomatal uptake when peak ozone concentrations occur in the air. This difference could also potentially be due to non-stomatal sinks being larger in midday than in the afternoon.

We conclude that stomatal uptake does not represent the major ozone sink for the orange orchard (Figs. 8 and 9), and only accounts for 20–45% of total daytime flux. In Fig. 11 we show median values of total ozone fluxes and all ozone sinks for the central hours of the day. Stomatal uptake did not exceed 31% of total ozone fluxes. We assumed in this work that ozone intercellular concentration is negligible (Laisk et al., 1989). However, stomatal ozone uptake may actually be lower than estimated because ozone concentration inside the stomata ($O3ci$) may be greater than zero. Laboratory studies using branch enclosures (Fares et al., 2010a), keeping constant the stomatal conductance, demonstrated indeed that this assumption is true only when ozone is at relative low ambient concentrations (~ 40 ppb). While $O3ci$ is slightly above zero at 100 ppb, it can reach considerable values of ~ 20 ppb when tropospheric ozone concentration is 140 ppb. This means that in summer, when we observed ozone levels above 100 ppb, an over-estimate of stomatal ozone fluxes may have occurred. Using the equation built with laboratory data, $O3ci = \exp(0.026 \cdot O3c)$, we found that in summer midday when ozone concentrations were

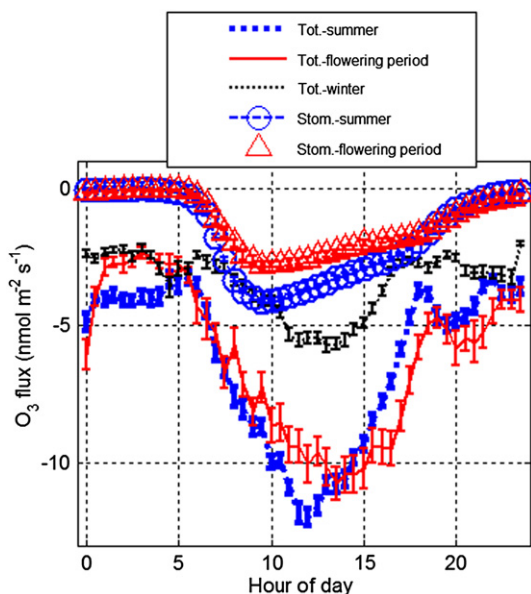


Fig. 9. Hourly average (\pm SD) of total and stomatal ozone fluxes for winter, flowering and summer periods.

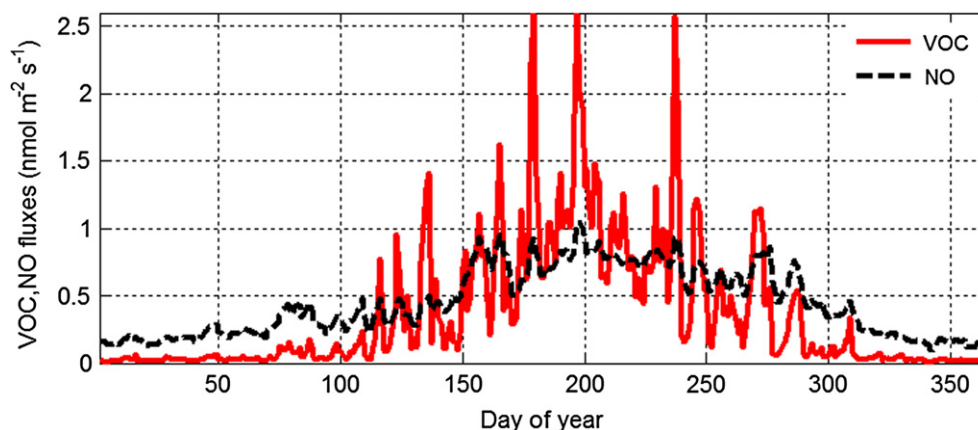


Fig. 10. Modeled BVOC and NO fluxes at 30-min time resolution.

above 100 ppb total stomatal ozone flux would have been overestimated by up to 10% because we did not account for non-zero O_3c_i .

3.5. Non-stomatal ozone deposition

Both the seasonal (Fig. 8) and diurnal average (Fig. 9) ozone fluxes show large differences between total and stomatal ozone fluxes, in agreement with previous studies which described high non-stomatal deposition processes (Kurpius and Goldstein, 2003; Hogg et al., 2007; Fares et al., 2010b). Here we explore how the non-stomatal portion of the ozone fluxes are likely partitioned in their various sinks.

Ozone flux to ground was estimated using the sum of in-canopy and ground resistances modeled with standard dry deposition algorithms. These calculations suggest that the ground compartment is a very important ozone sink, responsible for up to 35% of total ozone flux at midday. Ground deposition in our calculation was maximized at midday due to the diurnal concentration of ozone concentration peaking simultaneously with in-canopy resistances reaching their minimum ($<400 \text{ s m}^{-1}$) due to the higher levels of turbulence which promoted vertical mixing. High deposition rates to ground were expected at our field site, where there was significant open space between trees where the ground was exposed including soil particles, microorganisms, litter, and standing water. In our study, we assumed soil resistances were dependent on soil water content following the parameterization of Zhang et al. (2002) and Meszaros et al. (2009), although recent

studies have pointed out that relative humidity at the soil-level has greater influence than soil water content in the rate of ozone deposition on soils, since the increased adsorption of water molecules onto the ground reduces the availability of reaction sites for ozone (Stella et al., 2011). In our calculation, the magnitude of soil resistance changed in response to the cyclic irrigations which took place approximately every 5 days.

3.6. Ozone destruction via gas-phase chemistry: the role of BVOC and NO

The midday average non-stomatal ozone deposition in both the flowering and the summer period positively correlated with temperature (Fig. 5), suggesting that non-stomatal ozone fluxes are temperature dependent. This result is in agreement with previous research in forest ecosystems (Fares et al., 2010b; Kurpius and Goldstein, 2003; Mikkelsen et al., 2004). However, the low values of regression coefficients ($R^2 < 0.1$) suggest that in the orange orchard other relevant non-stomatal ozone sinks (e.g. deposition to ground) were present that were dependent on other factors such as humidity of soil and atmospheric turbulence.

As demonstrated by previous studies in different ecosystems, non-stomatal fluxes due to chemical reaction between ozone and VOC in the gas-phase can be important, and if not properly accounted for may lead to overestimations of stomatal fluxes in current chemical models (Oetl and Uhrner, 2011). We report in Fig. 10 daily averages of modeled fluxes of BVOC and NO. The emission of reactive BVOC is exponentially dependent on temperature due to volatilization of these molecules from storage organs (Kesselmeier and Staudt, 1999; Niinemets et al., 2004). In this work, we define reactive BVOC as those compounds for which the chemical time scale of the $\text{VOC}_x\text{-O}_3$ reaction is lower than the air retention time below the canopy, which we estimated to be ~ 4 min during midday when maximum vertical turbulence was occurring. Here we consider one sesquiterpene, β -caryophyllene, as the main reactive BVOC emitted from citrus (Fares et al., 2011; Ciccioli et al., 1999) which reacts with ozone in few seconds (Shu and Atkinson, 1994). The BEF values used in this research were previously measured in laboratory experiments under controlled conditions (Fares et al., 2011), although these emission estimates do not include soil, which may emit important additional amounts of BVOC (Ciccioli et al., 1999). Our assumption that one mol of BVOC reacts with one mol of ozone (Bouvier-Brown et al., 2009) is a conservative estimate considering that ozonolysis smog chamber tests have demonstrated that one molecule of a sesquiterpene with two or three double bonds reacts with more than one molecule of

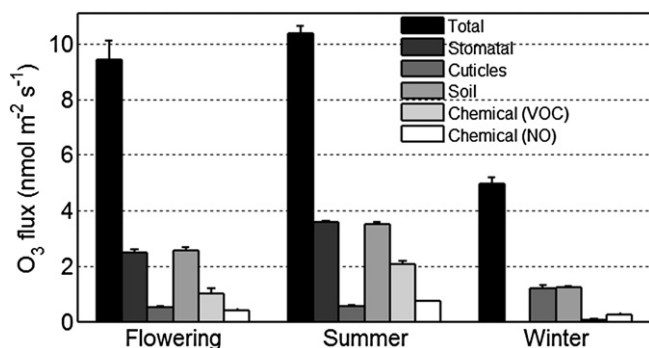


Fig. 11. Magnitude of total measured ozone flux and individually modeled ozone sinks, and the percentage of the total ozone flux represented by modeled stomatal, cuticle, soil, chemical VOC and chemical NO ozone sinks for winter, flowering and summer periods as daytime median values (10 AM–3 PM, \pm SD).

ozone generating several generations of oxidation products that contribute to formation of secondary organic aerosols (Shu and Atkinson, 1994). Overall, we estimate that chemistry in the gas phase was responsible for 10–26% of total ozone fluxes. This could be an underestimate if there are significant emissions of reactive BVOC in addition to β -caryophyllene that react with ozone before escaping the orchard. Given the nature of BVOC emitted (mostly terpenes) we exclude the possibility of fast ozone formation due to BVOC involvement in photochemical reactions.

Ozone is also known to be destroyed by reactions with NO molecules emitted from soil (Pilegaard, 2001; Kurpius and Goldstein, 2003; Farmer and Cohen, 2008). In the orange orchard, the amount of NO emission was probably enhanced because of fertilization, which resulted in both nitrification and also in NO release from denitrification (Sutton et al., 2009). Given the air retention time below and above the canopy which we estimated to be higher than the chemical time scale of the NO–O₃ reaction, ozone destruction by reaction with NO is expected, as documented by previous research (Nemitz et al., 2000; Duyzer et al., 1997; De Arellano et al., 1993). Soils of citrus orchards have been previously shown to be NO emitters (Matson and Mirestone, 1997). We are more confident of the BEF for BVOC, since we previously measured it for citrus species (Fares et al., 2011), while we are relying upon a BEF value for NO coming from the literature (2.4 g(N) m⁻² s⁻¹ Steinkamp and Lawrence, 2011) which may be an underestimation for citrus, a highly fertilized ecosystem. We assumed that 0.8 mol of ozone were removed for each mole of NO emitted from the soil following Kurpius and Goldstein, 2003. Ozone production is also enhanced when BVOC react to form HO₂ and RO₂ radicals which then react with NO, so the presence of reactive BVOC and NO emitted from soil also leads to ozone production above the canopy. Therefore, the assigned value of 0.8 does not consider later ozone formation above the canopy, thus relegating our estimate of ozone removal by NO to an “apparent ozone deposition” (Stella et al., 2011).

All of our estimates for individual components of ozone fluxes are compared to total observed ozone fluxes for flowering, summer, and winter periods in Fig. 11. During summer, the sum of individual sinks was 97% of the total measured flux, in good agreement with the measurements. For the flowering period, the individually estimated ozone sinks sum to 72% of the total measured flux, suggesting that we may have underestimated one or more sinks. During flowering carbon assimilation in *Citrus* decreases in favor of catabolic processes (Bustan and Goldschmidt, 1998; Fares et al., 2011), and a large amount of BVOC is emitted in the atmosphere from flowers to attract pollinators (Ciccioli et al., 1999; Dudareva and Pichersky, 2000; Fares et al., 2011). We hypothesize that the BVOC sink was underestimated during flowering because more reactive BVOC were emitted that were not included in our model of chemical ozone fluxes. In support of this conclusion are results (data not shown) from a year-long continuous flux measurement of less reactive BVOC (e.g. monoterpenes, methanol, acetone) which showed annual peaks of emission during the flowering period, and therefore displayed a different behavior than that modeled in Fig. 9. If we assume that the biosynthetic pathways for monoterpenes and reactive sesquiterpenes share the same precursors, a reasonable assumption in most cases, our hypothesis seems to rest on a sound basis. Anecdotal evidence for much larger BVOC emissions during this period is also available in the strong and beautiful aroma of the blossoming orange trees.

4. Conclusions

One entire year of measurements produced a robust dataset, which allowed us to investigate the absolute magnitude, seasonal

and diurnal cycles, and controls on ozone fluxes in a citrus orchard. We measured total ozone flux and separated it into stomatal and non-stomatal fluxes to assess the actual ozone flux into plants through stomata and the contributions to non-stomatal fluxes. Non-stomatal ozone sinks were shown to be the predominant pathways of ozone removal in the citrus orchard, with the dominant non-stomatal deposition occurring to ground and chemical reactions in the gas-phase with BVOC and NO.

We found that the citrus trees removed a considerable amount of tropospheric ozone over the year, similar in amount to that measured in a pine forest, thus suggesting that citrus orchards are ozone scavengers comparable in magnitude to forest ecosystems. Further work is necessary though to determine the net impact of orange orchards on regional ozone sources and sinks since this work did not assess the formation of ozone from BVOC emitted by the orchard.

Acknowledgments

We thank Jim and Milo Gorden for hosting this study in their orchard. Beth Grafton-Cardwell, Kurt Schmidt, and Dan Seymore of the UC Lindcove Station, and Rick Ramirez of UC Cooperative Extension provided critical support. We also thank Neil O'Connell and Craig Kallsen of UC Cooperative Extension. We gratefully acknowledge support for this research by the Citrus Research Board, the California Air Resources Board, and by the European Commission Marie Curie IOF 2008 project CITROVOC.

References

- Agriculture Commissioner reports. Citrus-growing areas in the San Joaquin Valley: Kern County, <http://www.kernag.com/caap/crop-reports/crop-reports.asp>, Tulare County, <http://agcomm.co.tulare.ca.us/default/index.cfm/crop-reports/>, Fresno County, <http://www.co.fresno.ca.us/fresnoag>.
- Altimir, N., Kolari, P., Tuovinen, J.P., Vesala, T., Bäck, J., Suni, T., Kulmala, M., Hari, P., 2006. Foliage surface ozone deposition: a role for surface moisture? *Biogeosciences* 3, 1–20.
- ARB, 2011. California Air Resources Board. <http://www.arb.ca.gov>.
- Bauer, M.R., Hultman, N.E., Panek, J.A., Goldstein, A.H., 2000. Ozone deposition to a ponderosa pine plantation in the Sierra Nevada Mountains (CA): a comparison of two different climatic years. *Journal of Geophysical Research* 105, 123–136.
- Bonachela, S., Orgaz, F., Villalobos, F.J., Fereres, E., 1999. Measurement and simulation of evaporation from soil in olive orchards. *Irrigation Science* 18, 205–211.
- Bouvier-Brown, N.C., Holzinger, R., Ollitzsch, K., Goldstein, A.H., 2009. Large emissions of sesquiterpenes and methyl chavicol quantified from branch enclosure measurements. *Atmospheric Environment* 43, 389–401.
- Bustan, A., Goldschmidt, E.E., 1998. Estimating the cost of flowering in a grapefruit tree. *Plant, Cell and Environment* 21, 217–224.
- California Irrigation Management Information System, <http://www.cimis.water.ca.gov/cimis/info.jsp>.
- Cape, J.N., Hamilton, R., Heal, M.R., 2009. Reactive uptake of ozone at simulated leaf surfaces: implications for ‘non-stomatal’ ozone flux. *Atmospheric Environment* 43, 1116–1123.
- Ciccioli, P., Brancaleoni, E., Frattoni, M., Di Palo, V., Valentini, R., Tirone, G., Seufert, G., Bertin, N., Hansen, U., Csik, O., Lenz, R., Sharma, M., 1999. Emission of reactive terpene compounds from orange orchards and their removal by within-canopy processes. *Journal of Geophysical Research* 104, 8077–8094.
- Cieslik, S., 2004. Ozone uptake by various surface types: a comparison between dose and exposure. *Atmospheric Environment* 38, 2409–2420.
- Cooper, O.R., Parrish, D.D., Stohl, A., Trainer, M., Nedelec, P., Thouret, V., Cammas, J.P., Oltmans, S.J., Johnson, B.J., Tarasick, D., Leblanc, T., McDermid, I.S., Jaffe, D., Gao, R., Stith, J., Ryerson, T., Aikin, K., Campos, T., Weinheimer, A., Avery, M.A., 2010. Increasing springtime ozone mixing ratios in the free troposphere over western North America. *Nature* 463, 344–348.
- De Arellano, J.V.G., Duykerke, P.G., Bultjes, P.J.H., 1993. The divergence of the turbulent diffusion flux in the surface layer due to chemical reactions: the NO–O₃–NO₂ system. *Tellus B* 45, 23–33.
- Dudareva, N., Pichersky, E., 2000. Biochemical and molecular aspects of floral scents. *Plant Physiology* 122, 627–634.
- Duyzer, J., Weststrate, H., Verhagen, H., Deinum, G., Baak, J., 1997. Measurements of dry deposition fluxes of nitrogen compounds and ozone. In: Slanina, S. (Ed.), 1997. Biosphere-atmosphere Exchange of Pollutants and Trace Substances: Experimental and Theoretical Studies of Biogenic Emissions and Pollutant Deposition, vol. 4. Springer, pp. 244–250.

- EPA, 2011. United States Environmental Protection Agency. Ozone air quality standards. <http://www.epa.gov/glo/standards.html>.
- Erismann, J.W., van Pul, A., Wyers, P., 1994. Parameterization of surface resistance for the quantification of atmospheric deposition of acidifying pollutants and ozone. *Atmospheric Environment* 28, 2595–2607.
- Fares, S., Barta, C., Brilli, F., Centritto, M., Ederli, L., Ferranti, F., Pasqualini, S., Reale, L., Tricoli, D., Loreto, F., 2006. Impact of high ozone on isoprene emission, photosynthesis and histology of developing *Populus alba* leaves directly or indirectly exposed to the pollutant. *Physiologia Plantarum* 128, 456–465.
- Fares, S., Loreto, F., Kleist, E., Wildt, J., 2008. Stomatal uptake and stomatal deposition of ozone in isoprene and monoterpene emitting plants. *Plant Biology* 10, 44–54.
- Fares, S., Park, J.H., Ormeno, E., Gentner, D.R., McKay, M., Loreto, F., Karlik, J., Goldstein, A.H., 2010a. Ozone uptake by citrus trees exposed to a range of ozone concentrations. *Atmospheric Environment* 44 (28), 3404–3412.
- Fares, S., McKay, M., Holzinger, R., Goldstein, A.H., 2010b. Ozone fluxes in a *Pinus ponderosa* ecosystem are dominated by non-stomatal processes: evidence from long-term continuous measurements. *Agricultural and Forest Meteorology* 150, 420–431.
- Fares, S., Goldstein, A., Loreto, F., 2010c. Determinants of ozone fluxes and metrics for ozone risk assessment in plants. *Journal of Experimental Botany* 61, 629–633.
- Fares, S., Gentner, D.R., Park, J.-H., Ormeno, E., Karlik, J., Goldstein, A.H., 2011. Biogenic emissions from Citrus species in California. *Atmospheric Environment* 45, 4557–4568.
- Farmer, D.K., Cohen, R.C., 2008. Forest nitrogen oxide emissions: evidence for rapid HOx chemistry within the canopy. *Atmospheric Chemistry and Physics* 8, 3899–3917.
- Feng, Z., Kobayashi, K., 2009. Assessing the impacts of current and future concentration of surface ozone on crop yield with meta-analysis. *Atmospheric Environment* 43, 1510–1519.
- Foken, T., Wichura, B., 1996. Tools for quality assessment of surface-based flux measurements. *Agriculture and Forest Meteorology* 78, 83–105.
- Ford, C., Goranson, C.E., Mitchell, R.J., Will, R.E., Teskey, R.O., 2004. Diurnal and seasonal variability in the radial distribution of sap flow: predicting total stem flow in *Pinus taeda* trees. *Tree Physiology* 24, 951–960.
- Gerosa, G., Dergli, F., Cieslik, S., 2007. Comparison of different algorithms for stomatal ozone flux determination from micrometeorological measurements. *Water Air Soil Pollution* 179, 309–321.
- Goldstein, A.H., Hultman, N.E., Fracheboud, J.M., Bauer, M.R., Panek, J.A., Xu, M., Qi, Y., Guenther, A.B., Baugh, W., 2000. Effects of climate variability on the carbon dioxide, water, and sensible heat fluxes above a ponderosa pine plantation in the Sierra Nevada (CA). *Agricultural and Forest Meteorology* 101, 113–129.
- Goldstein, A.H., McKay, M.A., Kurpius, M.R., Schade, G.W., Holzinger, R., 2004. Forest thinning experiment confirms ozone deposition to forest canopy is dominated by reaction with biogenic VOCs. *Geophysical Research Letters* 31, L22106.
- Granier, A., 1985. Une nouvelle méthode pour la mesure du flux de sève brute dans le tronc des arbres. *Annals of Forest Science* 42, 81–88.
- Granier, A., 1987. Evaluation of transpiration in a Douglas fir stand by means of sap flow measurements. *Tree Physiology* 3, 309–320.
- Guenther, A., Hewitt, C.N., Erickson, D., Fall, R., Geron, C., Graedel, T., Harley, P., Klinger, L., Lerdau, M., McKay, W.A., Pierce, T., Scholes, B., Steinbrecher, R., Tallamraju, R., Taylor, J., Zimmerman, P., 1995. A global model of natural volatile organic compounds emissions. *Journal of Geophysical Research* 100, 8873–8892.
- Hatton, T.J., Catchpole, E.A., Vertessy, R.A., 1990. Integration of sapflow velocity to estimate plant water-use. *Tree Physiology* 6, 201–209.
- Hogg, A., Uddling, J., Ellsworth, D., Carroll, M.A., Pressley, S., Lamb, B., Vogel, C., 2007. Stomatal and non-stomatal fluxes of ozone to a northern mixed hardwood forest. *Tellus* 59B, 514–525.
- Howard, C.J., Kumar, A., Malkina, I., Mitloehner, F., Green, P.G., Flocchini, R.G., Kleeman, M.J., 2010. Reactive organic gas emissions from livestock feed contribute significantly to ozone production in central California. *Environmental Science & Technology* 44, 2309–2314.
- Hsieh, C.I., Katul, G., Chi, T.W., 2000. An approximate analytical model for footprint estimation of scalar fluxes in thermally stratified atmospheric flows. *Advances in Water Resources* 23, 765–772.
- Kearney Agricultural Center. University of California, <http://soilstogo.uckac.edu>.
- Kesselmeier, J., Staudt, M., 1999. Biogenic volatile organic compounds (VOC): an overview on emission, physiology and ecology. *Journal of Atmospheric Chemistry* 33, 23–88.
- Kurpius, M.R., Goldstein, A.H., 2003. Gas-phase chemistry dominates O₃ loss to a forest, implying a source of aerosols and hydroxyl radicals to the atmosphere. *Geophysical Research Letters* 30.
- Kurpius, M.R., Panek, J.A., Nikolov, N.T., McKay, M., Goldstein, A.H., 2003. Partitioning of water flux in a Sierra Nevada ponderosa pine plantation. *Agricultural and Forest Meteorology* 117, 173–192.
- Laisk, A., Kull, O., Moldau, H., 1989. Ozone concentration in leaf intercellular air spaces is close to zero. *Plant Physiology* 90, 1163–1167.
- Lamaud, E., Carrara, A., Brunet, Y., Lopez, A., Druilhet, A., 2002. Ozone fluxes above and within a pine forest canopy in dry and wet conditions. *Atmospheric Environment* 36, 77–88.
- Lamaud, E., Loubet, B., Irvine, M., Stella, P., Personne, E., Cellier, P., 2009. Partitioning of ozone deposition over a developed maize crop between stomatal and non-stomatal uptakes, using eddy-covariance flux measurements and modelling. *Agricultural and Forest Meteorology* 149, 1385–1386.
- Loreto, F., Fares, S., 2007. Is ozone flux inside leaves only a damage indicator? Clues from volatile isoprenoid studies. *Plant Physiology* 143, 1096–1100.
- Massman, W.J., 1998. A review of the molecular diffusivities of H₂O, CO₂, CH₄, CO, O₃, SO₂, NH₃, N₂O, NO, and NO₂ in air, O₂ and N₂ near STP. *Atmospheric Environment* 32, 1111–1127.
- Matson, P., Mirestone, M., 1997. Agricultural Systems in the San Joaquin Valley: Development of Emission Estimates for Nitrogen Oxides. Report for the Air Research Board. <http://www.arb.ca.gov/research/apr/past/94-732.pdf> (last access on 03.08.11).
- Meszaros, R., Horvath, L., Weidinger, T., Neftel, A., Nemitz, E., Dammgen, U., Cellier, P., Loubet, B., 2009. Measurement and modelling ozone fluxes over a cut and fertilized grassland. *Biogeosciences* 6, 1987–1999.
- Mikkelsen, T.N., Ro-Poulsen, H., Hovmand, M.F., Jensen, N.O., Pilegaard, K., Egelov, A.H., 2004. Five-year measurements of ozone fluxes to a Danish Norway spruce canopy. *Atmospheric Environment* 38, 2361–2371.
- Monteith, J.L., Unsworth, M.H., 1990. Principles of Environmental Physics. Edward Arnold, London, pp. 291.
- Nemitz, E., Sutton, M.A., Wyers, G.P., Otjes, R.P., Schjørring, J.K., Gallagher, M.W., Parrington, J., Fowler, D., Choulaton, T.W., 2000. Surface/atmosphere exchange and chemical interaction of gases and aerosols over oilseed rape. *Agricultural and Forest Meteorology* 105, 427–445.
- Niinemets, U., Loreto, F., Reichstein, M., 2004. Physiological and physico-chemical controls on foliar volatile organic compound emissions. *Trends in Plant Science* 9, 180–186.
- Nowak, D.J., Crane, D.E., Stevens, J.C., 2006. Air pollution removal by urban trees and shrubs in the United States. *Urban Forestry and Urban Greening* 4, 115–123.
- Oetli, D., Uhrner, U., 2011. Development and evaluation of GRAL-C dispersion model, a hybrid Eulerian-Lagrangian approach capturing NO–NO₂–O₃ chemistry. *Atmospheric Environment* 45, 839–847.
- Parrish, D.D., Millet, D.B., Goldstein, A.H., 2009. Increasing ozone concentrations in marine boundary layer air inflow at the west coasts of North America and Europe. *Atmospheric Chemistry and Physics* 9, 1303–1323.
- Pilegaard, K., 2001. Air-soil exchange of NO, NO₂ and O₃ in forests. *Water Air and Soil Pollution* 1, 79–88.
- Pleijel, H., Pihl Karlsson, G., Danielsson, H., 1995. Surface wetness enhances ozone deposition to a pasture canopy. *Atmospheric Environment* 29, 3391–3393.
- Rissmann, J., Tetzlaff, G., 1994. Application of a spectral correction method for measurements of covariances with fast-response sensors in the atmospheric boundary layer up to a height of 130 m testing of the corrections. *Boundary-Layer Meteorology* 70, 293–305.
- Shu, Y., Atkinson, R., 1994. Rate constants for the gas-phase reactions of O₃ with a series of terpenes and OH radical formation from the O₃ reactions with sesquiterpenes at 296 K. *International Journal of Chemical Kinetics* 26, 1193–1205.
- Steiner, A.L., Tonse, S., Cohen, R.C., Goldstein, A.H., Harley, R.A., 2006. The influence of future climate and emissions on regional air quality in California. *Journal of Geophysical Research* 111, D18303. doi:10.1029/2005JD006935.
- Steinkamp, J., Lawrence, M.G., 2011. Improvement and evaluation of simulated global biogenic soil NO emissions in an AC-GCM. *Atmospheric Chemistry and Physics* 11, 6063–6082.
- Stella, P., Loubet, B., Lamaud, E., Laville, P., Cellier, P., 2011. Ozone deposition onto bare soil: a new parameterization. *Agricultural and Forest Meteorology* 151, 669–681.
- Sutton, M.A., Nemitz, E., Theobald, M.R., Milford, C., Dorsey, J.R., Gallagher, M.W., Hensen, A., Jongejans, P.A.C., Erismann, J.W., Mattsson, M., Schjørring, J.K., Cellier, P., Loubet, B., Roche, R., Neftel, A., Hermann, B., Jones, S.K., Lehman, B.E., Horvath, L., Weidinger, T., Rajkai, K., Burkhardt, J., Löpmeier, F.J., Daemmgen, U., 2009. Dynamics of ammonia exchange with cut grassland: strategy and implementation of the GRAMINAE Integrated Experiment. *Biogeosciences* 6, 309–331.
- Taha, H., 1996. Modeling impacts of increased urban vegetation on ozone air quality in the South Coast Air Basin. *Atmospheric Environment* 30, 3423–3430.
- Turnipseed, A.A., Burns, S.P., Moore, D.J.P., Hu, J., Guenther, A.B., Monson, R.K., 2009. Controls over ozone deposition to a high elevation subalpine forest. *Agricultural and Forest Meteorology* 149, 1447–1459.
- UNECE, 2004. Revised Manual on Methodologies and Criteria for Mapping Critical Levels/loads and Geographical Areas where they are Exceeded (2004). www.icpmapping.org.
- Van Dingenen, R., Dentener, F.J., Raes, F., Krol, M.C., Emberson, L., Cofala, J., 2009. The global impact of ozone on agricultural crop yields under current and future air quality legislation. *Atmospheric Environment* 43, 604–618.
- Vingarzan, R., 2004. A review of surface ozone background levels and trends. *Atmospheric Environment* 38, 3431–3442.
- Vollenweider, P., Gunthardt-Goerg, M.S., 2005. Diagnosis of abiotic and biotic stress factors using the visible symptoms in foliage. *Environmental Pollution* 137, 455–465.
- Wilczak, J.M., Oncley, S.P., Stage, S.A., 2001. Sonic anemometer tilt correction algorithms. *Boundary-Layer Meteorology* 99, 127–150.
- Wittig, V.E., Ainsworth, E.A., Naidu, S.L., Karnosky, D.F., Long, S.P., 2009. Quantifying the impact of current and future tropospheric ozone on tree biomass, growth, physiology and biochemistry: a quantitative meta-analysis. *Global Change Biology* 15, 396–424.
- Yienger, J.J., Levy, H., 1995. Empirical model of global soil-biogenic NO_x emissions. *Journal of Geophysical Research* 100, 11447–11464.
- Zhang, L., Brook, J.R., Vet, R., 2002. On ozone dry deposition—with emphasis on non-stomatal uptake and wet canopies. *Atmospheric Environment* 36, 4787–4799.
- Zhang, L., Brook, J.R., Vet, R., 2003. A revised parameterization for gaseous dry deposition in air-quality models. *Atmospheric Chemistry and Physics* 3, 2067–2082.